J Neuropathol Exp Neurol
Vol. 75, No. 2, February 2016, pp. 134–147
doi: 10.1093/jnen/nlv012

ORIGINAL ARTICLE

Progenitor/Stem Cell Markers in Brain Adjacent to Glioblastoma: GD3 Ganglioside and NG2 Proteoglycan Expression

Gina Lama, ScD, Annunziato Mangiola, MD, Gabriella Proietti, ScD, Anna Colabianchi, PhD, Cristiana Angelucci, PhD, Alessio D'Alessio, PhD, Pasquale De Bonis, PhD, Maria Concetta Geloso, PhD, Libero Lauriola, MD, Elena Binda, PhD, Filippo Biamonte, PhD, Maria Grazia Giuffrida, ScD, Angelo Vescovi, PhD, and Gigliola Sica, MD

Abstract

Characterization of tissue surrounding glioblastoma (GBM) is a focus for translational research because tumor recurrence invariably occurs in this area. We investigated the expression of the progenitor/stem cell markers GD3 ganglioside and NG2 proteoglycan in GBM, peritumor tissue (brain adjacent to tumor, BAT) and cancer stem-like cells (CSCs) isolated from GBM (GCSCs) and BAT (PCSCs). GD3 and NG2 immunohistochemistry was performed in paired GBM and BAT specimens from 40 patients. Double-immunofluorescence was carried out to characterize NG2-positive cells of vessel walls. GD3 and NG2 expression was investigated in GCSCs and PCSCs whose tumorigenicity was also evaluated in *Scid/bg* mice. GD3 and NG2 expression was higher in tumor tissue than in BAT. NG2 decreased as the distance from tumor margin increased, regardless of the tumor cell presence, whereas GD3 correlated with neoplastic infiltration. In BAT, NG2 was coexpressed with α-smooth muscle actin (α-SMA) in pericytes and with nestin in the endothelium. Higher levels of NG2 mRNA and protein were found in GCSCs while GD3 synthase was expressed at similar levels in the 2 CSC populations. PCSCs had lower tumorigenicity than GCSCs. These data suggest the possible involvement of GD3 and NG2 in pre/pro-tumorigenic events occurring in the complex microenvironment of the tissue surrounding GBM.

Institute of Histology and Embryology (GL, GP, AC, CA, ADA, FB, GS); Institute of Neurosurgery (AM), "A. Gemelli" Faculty of Medicine, Catholic University of the Sacred Heart, Rome, Italy; Neurosurgery, "S. Anna" University Hospital (PDB), Cona di Ferrara, Italy; Institute of Anatomy and Cell Biology (MCG); Institute of Pathology (LL), "A. Gemelli" Faculty of Medicine, Catholic University of the Sacred Heart, Rome, Italy; IRCCS Casa Sollievo della Sofferenza (EB), c/o Istituto Mendel, Rome, Italy; IRCCS Casa Sollievo della Sofferenza (MGG, AV), San Giovanni Rotondo, Foggia, Italy; Department of Biological Sciences and Biotechnology (AV), University of Milano-Bicocca, Milan, Italy.

Send correspondence to: Gigliola Sica, Institute of Histology and Embryology, "A. Gemelli" Faculty of Medicine, Catholic University of the Sacred Heart, Largo F. Vito, 1, 00168-Rome, Italy; E-mail: gigliola@rm.unicatt.it

This research was supported by a grant from the MIUR FIRB "Accordi di Programma" 2010 (RBAP10KJC5_003).

Supplementary Data can be found at http://www.jnen.oxfordjournals.org.

Key Words: Glioblastoma, Brain adjacent to tumor, Cancer stem cells, GD3 ganglioside, NG2 proteoglycan.

INTRODUCTION

Molecular characterization of glioblastomas (GBM) has provided a great deal of data on genetic alterations (1), specific biomarkers (2), and proliferation pathways (3), which have proven marginally relevant for disease management or outcome prediction. Because tumor recurrence occurs in tissue neighboring GBM in approximately 90% of patients (even after maximal surgical resection followed by radiotherapy and chemotherapy), these areas are assuming growing relevance in translational research (4, 5). Indeed, the brain adjacent to tumor (BAT) shows edema, vascular alterations (6, 7), reactive astrocytes and microglia (8, 9), abnormal levels of various elements, amino acids, signal transducers, activators of transcription proteins, and other molecules (10–13), indicating that complex changes occur in close proximity to the edges of GBM. In previous studies, we have shown that phosphorylated (p) ERK1/2 and pJNKs, which are known to be involved in cell growth, differentiation, motility, and apoptosis, are equally expressed in GBM and in the surrounding tissue, where they are also present independently of neoplastic cells (14, 15). Nestin, a well-known protein marker of embryonic and adult stem/progenitor cells (16, 17), correlates with the glioma grade, is highly expressed in the majority of GBM cells and is rarely detectable in BAT (15). Moreover, the pJNK/nestin ratio, measured at a distance <1 cm from the tumor margin, is correlated with a longer median patient survival time (15). All of these markers have been observed in reactive glial cells and apparently normal cells as well as in the vessel walls in BAT. We have also shown that endothelial cells in GBM and BAT are characterized by expression of CD105, an accessory receptor for transforming growth factor-β superfamily ligands; CD105 is a known proliferation-associated and hypoxia-inducible protein that marks activated endothelium of tumor vessels (18). It is remarkable that the blood vessel morphology outside the tumor is quite similar to that of GBM microvessels, showing

hypertrophic endothelial cells protruding into the lumen and a significant number of α-SMA-positive pericytes. Moreover, the microvessel density evaluated by CD105 expression in the tissue located at a distance >1 cm from the GBM margin correlates with GBM patient survival (19). More recently, molecular analysis of both GBM and BAT apparently free of tumor cells revealed significant changes in the expression of 1323 genes. Among the dysregulated genes in BAT, 15 were upregulated, whereas 42 were downregulated compared with normal white matter. In addition, cells positive for CD133, which is widely considered as a putative biomarker of CSCs in brain tumors, were found in this area (20, 21). The expression of stem-cell markers (eg, nestin and CD133) in apparently normal cells of BAT led us to hypothesize of a close phenotypic relationship with CSCs. On the other hand, it has been reported that both GBM and BAT contain CSCs showing distinct characteristics that include genetic anomalies, tumorigenic ability, and self-renewal (22).

To define the molecular characteristics of the GBM neighboring tissue better and to identify tumor markers potentially useful for developing future therapeutic targets, we investigated the expression of the GD3 ganglioside and the transmembrane NG2 chondroitin sulphate proteoglycan. In GBM, these progenitor/stem-cell markers are important for tumor cell proliferation, migration/invasion, and survival, as well as angiogenesis, and for identifying a cell population with an aggressive molecular signature that plays a crucial role in inducing tumor cell proliferation (2, 23–26). Moreover, to confirm the altered status of BAT, which is apparently not infiltrated, we analyzed abnormalities of cell cycle-related molecules distinctive of different tumors, including GBM. In particular, we explored the expression of the proliferation marker Ki67, the deletion of phosphatase and tensin homolog (*PTEN*), a critical negative regulator in growth control (27), and the amplification of mouse double minute 2 homolog (*MDM2*), an important negative regulator of the tumor suppressor gene *p53* (28). Finally, to improve the understanding of the stem cell elements that are present in the BAT, the expression of GD3, NG2, and Ki67 was also investigated in CSCs isolated from GBM (GCSCs) and from BAT (PCSCs) of primary GBM patients.

MATERIALS AND METHODS

Patients and Tissue Samples

This study involved 40 adult patients with primary supratentorial GBM who underwent "en bloc" surgery at the Institute of Neurosurgery of the Catholic University of the Sacred Heart in Rome, Italy. GBMs were considered as primary based on the patients' clinical history, very short time-interval between first symptoms or signs of disease, admission to hospital, and a rapid clinical progression. Neuronavigation and intraoperative ultrasound were used to define and maximize the extent of intracranial tumor resection. The surgical specimens were cut and opened in a "book-wise" fashion. Using this technique, the difference between tumor border and its surrounding apparently normal white matter was evident, and the distance from white matter adjacent to tumor edge was well defined and measured (29). In all patients, early contrast magnetic resonance imaging (MRI) within 24 to 48 hours after surgery, comparing pre- and post-operative contrast-enhanced images, confirmed the complete removal of the enhanced lesion (T1-weighted zone) and the extension of the resection (T2- weighted MRI zone).

Paired GBM and BAT tissue samples of each patient were obtained from the enhanced lesion without areas of necrosis (tumor) and from the white matter at a distance <1 cm (BAT 1) and between 1 and 3.5 cm (BAT 2) from the macroscopic tumor border. The larger resections were done in tumors growing far from eloquent areas. Nevertheless, the anatomic location of the tumors did not always allow sampling from the 3 areas. Thus, 40 paraffin-embedded tissue specimens were derived from the tumor, 34 from BAT 1, and 23 from BAT 2. Specimens from these areas were assessed histologically by an expert pathologist. As previously described (30), white matter-invading GBM cells were identified by means of their nuclear atypia and heteropyknotic staining, which was similar to that of the cells within the tumor core. Reactive astrocytes were discriminated through their distinct stellate morphology with eosinophilic cytoplasm and large, eccentric, round nuclei. Fewer frozen tissue samples were obtained from the 3 areas (15 from the tumor, 15 from BAT 1 and 7 from BAT 2). All samples were from patients who had received no prior treatment. Thirty-five days after surgery (range: 30-40 days), patients underwent irradiation and chemotherapy performed according to standard protocols (31). The survival period was defined as the time elapsed from the date of surgery to the date of death. Non-tumor brain specimens containing histologically normal white matter were obtained from 4 patients at the same ages operated for deep cavernomas with radiological signs of recent bleeding. These were used as controls in immunohistochemistry and molecular analyses. The study was approved by Ethics Committee of the Catholic University of the Sacred Heart, Rome, Italy (Prot. A/205/2011). All patients gave informed written consent to use tumor, BAT, and control tissue as well as clinical data for research purposes.

Isolation, Characterization and *In Vivo* Tumorigenicity of GBM and BAT Stem Cells

Fresh surgical tumor and BAT specimens (at a distance ≥1cm from macroscopic border), derived from 4 patients, were dissected and digested in papain solution (Worthington Biochemical, Lakewood, NJ). Primary cells were plated and cultured at clonal density in neural stem cell medium: serum-free NeuroCult NS-A Basal Medium supplemented with NeuroCult NS-A Proliferation Supplement, 20 ng/ml EGF, 10 ng/ml bFGF and 0.2% heparin (StemCell Technologies, Vancouver, Canada) (32). This procedure was used to isolate, from adult GBM and BAT, a subset of cells that formed neurospheres that reproducibly established long-term expanding cell lines, proved to be multipotent and were capable of unlimited self-renewal.

Population analysis and differentiation experiments were performed using reported methods (33). To evaluate the tumorigenic activity, 3 μl of 1 x 10^5 GCSCs or PCSCs/μl solution in phosphate buffered saline was injected intracranially into the right striatum of *Scid/bg* mice (Charles River Laboratories Italia, Lecco, Italy), as previously described (32). All animal procedures were conducted in accordance with the *Guidelines*

for the Care and Use of Laboratory Animals and were approved by the Institutional Animal Care and Use Committees at the University of Milano-Bicocca.

Immunohistochemistry

Formalin-fixed paraffin-embedded tissue sections (5 μm) from GBM and BAT samples of 40 patients were used for GD3 and Ki-67 immunohistochemical staining. After deparaffinization and hydration, endogenous peroxidase was blocked by incubation with 3% H_2O_2. After blocking with Super Block (UCS Diagnostic, Morlupo, Italy) of non-specific staining, the sections were incubated with mouse anti-human monoclonal antibodies against GD3 (clone VIN-IS-56, diluted 1:30, Chemicon International Inc., Temecula, CA), Ki-67 (clone MIB-1, diluted 1:100, Dako, Glostrup, Denmark), or glial fibrillary acidic protein (GFAP, clone 6F2, diluted 1:500, Dako).

NG2 staining was performed on 10-μm-thick frozen tissue sections from GBM and BAT of 15 patients. The cryostat sections were air-dried and fixed in 4% paraformaldehyde for 10 minutes. After quenching of endogenous peroxidase activity and blocking of non-specific binding, sections were incubated with the rabbit anti-human polyclonal antibody against NG2 (diluted 1:200, Chemicon International). All samples were then incubated with a horseradish peroxidase (HRP) polymer conjugate against mouse and rabbit secondary antibodies (SuperPicture Polymer, Invitrogen, Carlsbad, CA). Staining was completed by incubation with DAB (3,3-diaminobenzidine) plus substrate-chromogen (Peroxidase DAB substrate Kit, Vector Laboratories Inc., Burlingame, CA), which resulted in a red-brown signal indicating GD3 and NG2 expression. Finally, nuclei were lightly counterstained with Mayer's hematoxylin. Two sections of each area were examined by 2 independent observers using a light microscope (Axioskop 2 plus, Zeiss, Jena, Germany). At least 1000 to 2500 cells from 4 to 10 randomly selected fields in each section were counted at x400 magnification, to assess the presence or absence of GD3 and NG2. The few cases with discrepant scoring were reevaluated jointly and agreement was reached. The percentage of positive cells was calculated and reported as average ± SD. All immunolabeled cells, excluding endothelial cells, were counted.

Immunofluorescence and Confocal Microscopy

To characterize NG2-positive cells, double staining experiments were performed using immunofluorescence and confocal microscopy. Frozen sections from GBM and BAT samples were blocked with Super Block and incubated with the anti-NG2 antibody (diluted 1:200), followed by incubation with secondary antibody (donkey anti-rabbit Cy2; diluted 1:200; Jackson ImmunoResearch Laboratories, West Grove, PA) conjugated with green fluorochrome. The sections were then washed and incubated again with the mouse primary monoclonal antibodies anti-CD105 (clone SN6h, diluted 1:10, DakoCytomation Inc., Carpinteria, CA) or anti-nestin (clone 10C2, diluted 1:200, Millipore, Darmstadt, Germany), or anti-α-SMA (clone HHF35, diluted 1:100, DakoCytomation, Inc.). Subsequently, incubation with the secondary antibody (donkey anti-mouse Cy3; diluted 1:200, Jackson ImmunoResearch Laboratories) conjugated with red fluorescent cyanine was performed. The colocalization of the different markers was examined with a confocal laser scanning microscopy system (Zeiss LSM 510 META, Oberkochen, Germany).

Immunocytochemistry

GCSC and PCSC neurospheres derived from 4 patients were fixed in 4% paraformaldehyde, cryoprotected in 30% sucrose, snap-frozen in liquid nitrogen, and stored at –80°C until use. Frozen sections (10 μm) were evaluated by immunocytochemical staining for the expression of GD3, NG2, and Ki-67, as described in the Immunohistochemistry section.

Double immunofluorescence staining was performed on GCSCs and PCSCs. Sections were blocked with Super Block and incubated with the anti-NG2 antibody (diluted 1:200) followed by incubation with secondary donkey anti-rabbit Alexa Fluor 594 (diluted 1:5000; Life Technologies, Eugene, OR). The sections were then washed and incubated again with the mouse primary monoclonal antibody anti-GD3 (clone VIN-IS-56, diluted 1:30). Subsequently, incubation with secondary donkey anti-mouse Alexa Fluor 488 (diluted 1:5000; Life Technologies) was performed. The nuclei were stained with DAPI (Prolong Gold anti-fade reagent with DAPI, Life Technologies). The colocalization of the 2 markers was examined with the fluorescent microscope Olympus BX53 with UIS2 optical system.

Fluorescence *In Situ* Hybridization

In tissue samples derived from GBM and BAT from 4 patients (2 with and 2 without tumor cells), fluorescence *in situ* hybridization (FISH) was carried out to verify on chromosome 10q23.31 the deletion of *PTEN* (RP11-302L4 probe), and on chromosome 12q15 the amplification of *MDM2* (RP11-77H17 probe) genes as tumor cell molecular markers. FISH analyses were performed on nuclei isolated from 2 20-μm sections for each formalin-fixed paraffin-embedded tissue sample, as previously described with minor modifications (34). All BAC (bacterial artificial chromosome) clones were purchased from Source BioScience (Nottingham, UK). Bacterial DNA was extracted by using the Plasmid Kit Miniprep Q-Spin (VWR International, West Chester, PA) according to the manufacturers' protocol. The RP11-316L10 clone, mapping to 22q11.21, was used as control and was labeled together to RP11-302L4 or RP11-77H17. Labeling in dual-color was performed using the Nick Translation Kit (Abbott Laboratories, Abbott Park, IL), using SpectrumOrange and SpectrumGreen dUTP.

The nuclei were counterstained with DAPI/Vectashield antifade solution (Vector Laboratories, Inc.). An Eclipse 80i fluorescence microscope equipped with a computerized system (Genikon; Nikon, Florence, Italy) was used to acquire and examine images. Fifty consecutive interphase nuclei from GBM and 50 from both BAT 1 and 2 of each patient were analyzed by 2 microscopists in masked fashion.

Western Blot Analysis

To evaluate the expression of GD3 synthase and NG2 protein, immunoblotting was performed on GCSCs and PCSCs of 4 patients. Cells were lysed with cell lysis buffer (150 mM NaCl, 1% Nonidet P-40, 0.5% Triton X-100, 0.5 mM EDTA, 0.1% SDS, 50 mM Tris-HCl, pH 7.6) containing protease and phosphatase inhibitor cocktails (Sigma-Aldrich) supplemented with 17.4 μg/ml PMSF (Sigma-Aldrich). Proteins in the lysates were quantified by Bradford Protein Assay. Twenty-five μg of total proteins were fractioned by 8% to 10% SDS-PAGE, transferred electrophoretically to a PVDF membrane (Immobilon-P Transfer Membrane, Millipore, Bedford, MA), and immunoblotted with primary rabbit polyclonal antibodies against GD3 synthase (diluted 1:200, Santa Cruz Biotechnology, Inc., Santa Cruz, CA) or NG2 (diluted 1:1000, Millipore). Membranes were then incubated with HRP-conjugated antibodies (diluted 1:160000, Sigma-Aldrich). Detection of the bound antibody by enhanced chemiluminescence was performed using Immun-Star WesternC Chemiluminescence Kit (Bio-Rad Laboratories Inc., Hercules, CA), according to the manufacturer's instructions. Membranes were reprobed with an anti β-actin monoclonal antibody (diluted 1:5000, Sigma-Aldrich) as an internal control for protein loading. The signals were quantitated by densitometry (Chemi Doc Documentation System/Quantity One quantitation software, Bio-Rad). Densitometry units of the protein of interest were then corrected for the densitometry units of β-actin.

Quantitative Real Time PCR Analysis

Quantitative real time PCR (qPCR) analysis was carried out on both GCSCs and PCSCs to determine mRNA of GD3 synthase and NG2. Total RNA was extracted with the RNAqueous-4PCR kit (Ambion Inc., Austin, TX), according to the manufacturer's instructions. Three μg of RNA were converted into single-stranded DNA by a standard 50-μl RT reaction with the TaqMan RT Reagent (Life Technologies, Carlsbad, CA). The cDNA generated from the reverse transcription reactions was amplified by PCR with the SYBR Green Supermix (Quantace, London, UK) in a total volume of 25 μl. The samples were incubated at 94°C for 2 minutes, 94°C for 30 seconds, 53°C for 30 seconds and 72°C for 30 seconds, for 40 cycles on a StepOne Real-Time PCR Systems (Life Technologies). The primers used were as follows: NG2, 5-TTTCCGTGTCACAGCTCCACCATA-3 and 5'-AGCTGGCACTGTTGAGACTCTTGA-3'; GD3 synthase, 5'-TGGAGCTGGACCCATGTGAAGATA-3' and 5'-AGGGCCCATGCAAACTCAT GAAAC-3'; β-actin, 5'-AA TGTGGCCGAGGACTTTGATTGC-3' and 5'-AGGATGG CAAGGGACTTCCTGTAA-3'. The level of messenger RNA of NG2 and GD3 synthase was expressed as relative fold-change versus the β-actin messenger RNA. The $2^{-\Delta\Delta Ct}$ method was used to calculate real time PCR results (35) where $^{\Delta\Delta}Ct = {}^{\Delta}Ct$ (PCSCs) - $^{\Delta}Ct$ (GCSCs); $^{\Delta}Ct = Ct$ (target gene) - Ct (β-actin). Reactions were performed in triplicate.

Statistical Analysis

The statistical analyses were carried out using SPSS software package for Windows (version 15.0.1 SPSS, Inc., Chicago, IL). Since the expression levels of variables considered were not normally distributed, non-parametric tests were applied to find statistically significant differences among groups. The Kruskal-Wallis test was used to compare the GD3 or NG2 expression among GBM, BAT 1 and BAT 2. To find differences in GD3 or NG2 expression between 2 areas (GBM vs. BAT 1; GBM vs. BAT 2; BAT 1 vs. BAT 2), the Mann-Whitney (unpaired data) and the Wilcoxon Signed Rank (paired data) tests were used. Patient and mice survival time was analyzed with the Kaplan-Meier method and the log-rank (Mantel-Cox) test was used to compare the differences between groups. In patients, the correlation between age groups (<65 and ≥ 65 years), gender, Karnofsky performance status (KPS) (KPS = 80 and KPS = 90–100), GD3 expression, and survival was analyzed. In particular, in each area the median value of GD3 expression was used as a cut-off point to dichotomize the patients in 2 groups. To evaluate the significance of the difference in GD3 synthase or NG2 expression level between GCSCs and PCSCs, an unpaired two-tailed Student t-test was used. An α level of less than 0.05 ($p < 0.05$) was used for statistical significance in all tests.

RESULTS

Patient Characteristics

The clinicopathological characteristics of patients are presented in Table 1, including 21 female and 19 male patients; their ages ranged from 20 to 75 years (mean: 59.3). All patients had a KPS of ≥ 70.

GD3 and NG2 Are Expressed in Tumor and BAT of Human GBM

The expression of GD3 was detected in both GBM and BAT. GD3 staining was seen in the cytoplasm of tumor cells (Fig. 1A, B) and endothelial cells (Fig. 1 D-F). Moreover, GD3 immunostaining was present in apparently normal cells (Fig. 1C) and reactive astrocytes of BAT (Fig. 1F). The Kruskal-Wallis test showed a difference in GD3 expression among the 3 areas ($p < 0.001$). The proportion of GD3 expressing cells was higher in GBM (14.34 ± 12.62) than in BAT 1 (4.43 ± 4.67) and BAT 2 (4.16 ± 4.19) ($p < 0.001$, Mann-Whitney and Wilcoxon Signed Rank tests). No significant difference was found in the GD3 levels between the 2 areas surrounding the neoplasia, but GD3 expression in both BAT 1 and BAT 2 was higher when tumor cells were present ($p < 0.005$, Mann-Whitney test) (Table 2). NG2 immunoreactivity was found in both GBM and BAT; the staining was localized in the cytoplasm not only in neoplastic cells (Fig. 1G, H), but also in glial cells with various morphologies (Fig. 1I).

NG2 was expressed in vascular cell population in GBM and in BAT (Fig. 1J-L). The Kruskal-Wallis test showed a difference in NG2 expression among the 3 areas ($p < 0.001$). The percentage of NG2-positive cells was higher in GBM (23.81 ± 6.50) than in BAT 1 (12.44 ± 8.34) ($p < 0.01$, Mann-Whitney and Wilcoxon Signed Rank tests) and in BAT 2 (4.64 ± 3.61) ($p < 0.001$ Mann-Whitney test; $p < 0.05$ Wilcoxon Signed Rank test). NG2 immunoreactivity decreased from BAT 1 to BAT 2, and a significant difference was

TABLE 1. Clinicopathological Characteristics of the 40 Adult Patients With Primary Glioblastoma

Patient No.	Gender	Age at Diagnosis (years)	Tumor Localization	KPS Score	Treatment	Survival Time (months)	Clinical Outcome
1	M	67	Parieto-temporal	80	RT+CH	8	DOD
2	M	63	Frontal	100	RT+CH	11	DOD
3	F	47	Frontal	100	RT+CH	14	DOOC
4	F	65	Parieto-occipital	80	RT+CH	18	DOD
5	F	58	Frontal	100	RT+CH	15	DOD
6	F	71	Frontal	80	RT+CH	13	DOD
7	F	61	Frontal	100	RT+CH	12	DOD
8	M	58	Parieto-temporal	80	RT+CH	19	DOD
9	M	72	Parietal	90	RT+CH	12	DOD
10	M	43	Parietal	80	RT+CH	19	DOD
11	F	68	Frontal	90	RT+CH	28	DOD
12	F	49	Frontal	100	RT+CH	59	DOD
13	F	47	Frontal	100	RT+CH	25	DOD
14	F	65	Frontal	90	–	2	DOOC
15	M	69	Frontal	70	–	0,1	DOOC
16	M	71	Parietal	80	RT+CH	22	DOD
17	M	61	Frontal	100	RT+CH	13	DOOC
18	F	72	Parieto-temporal	90	RT+CH	15	DOD
19	F	62	Fronto-temporal	80	RT+CH	14	DOD
20*	M	44	Frontal	100	RT+CH	19	DOD
21*	F	72	Frontal	80	–	0.2	DOOC
22	F	72	Frontal	80	RT+CH	6	DOD
23*	M	68	Temporal	80	–	3	DOD
24*	M	51	Temporal	100	RT+CH	9	DOD
25	M	42	Temporal	80	RT+CH	39	DOD
26	M	52	Parieto-temporal	80	RT+CH	13	DOD
27	F	49	Parieto-occipital	90	RT+CH	8	DOD
28	F	52	Temporal	90	RT+CH	35	DOD
29	M	20	Parieto-temporal	100	RT+CH	28	DOD
30*	M	71	Fronto-temporal	90	RT+CH	5	DOD
31*	M	75	Parietal	80	RT+CH	6	DOD
32*°	F	59	Temporal	100	RT+CH	10	DOD
33*	F	71	Frontal	100	RT+CH	9	DOD
34*	F	43	Parieto-occipital	100	RT+CH	53	DOD
35*	M	51	Parieto-temporal	90	RT+CH	38	DOD
36*	M	69	Temporal	80	RT+CH	19	DOD
37*	F	63	Temporal	90	RT+CH	12	DOD
38*°	F	50	Frontal	80	RT+CH	31	DOOC
39*°	M	67	Temporal	90	RT+CH	13	DOD
40*°	F	62	Frontal	80	RT+CH	7	DOD

CH, chemotherapy; DOD, dead of disease; DOOC, dead of other causes; F, female; KPS, Karnofsky performance status; M, male; RT, radiotherapy. Paraffin-embedded tissue sections were obtained from patients #1-40.

*Patients from whom frozen sections were obtained.

°Patients from whom glioblastoma cancer stem-like cells (GCSCs) and cancer stem-like cells from brain adjacent to glioblastoma (PCSCs) were isolated.

found between the 2 BAT regions ($p < 0.01$ Mann-Whitney test; $p < 0.05$, Wilcoxon Signed Rank test). NG2 expression level in BAT was independent of the presence of neoplastic cells. In controls, GD3 and NG2 were not detected, whereas GFAP expression was localized in the cytoplasm of astrocytes (Supplementary Data - Figure 1).

NG2, CD105, α-SMA and Nestin Are Expressed in Vessel Walls

Double-label fluorescent immunohistochemistry of GBM and BAT revealed NG2 immunostaining adjacent to CD105-positive endothelium in cells that are most likely pericytes (Fig. 2C, F). Their identity as pericytes was demonstrated by the

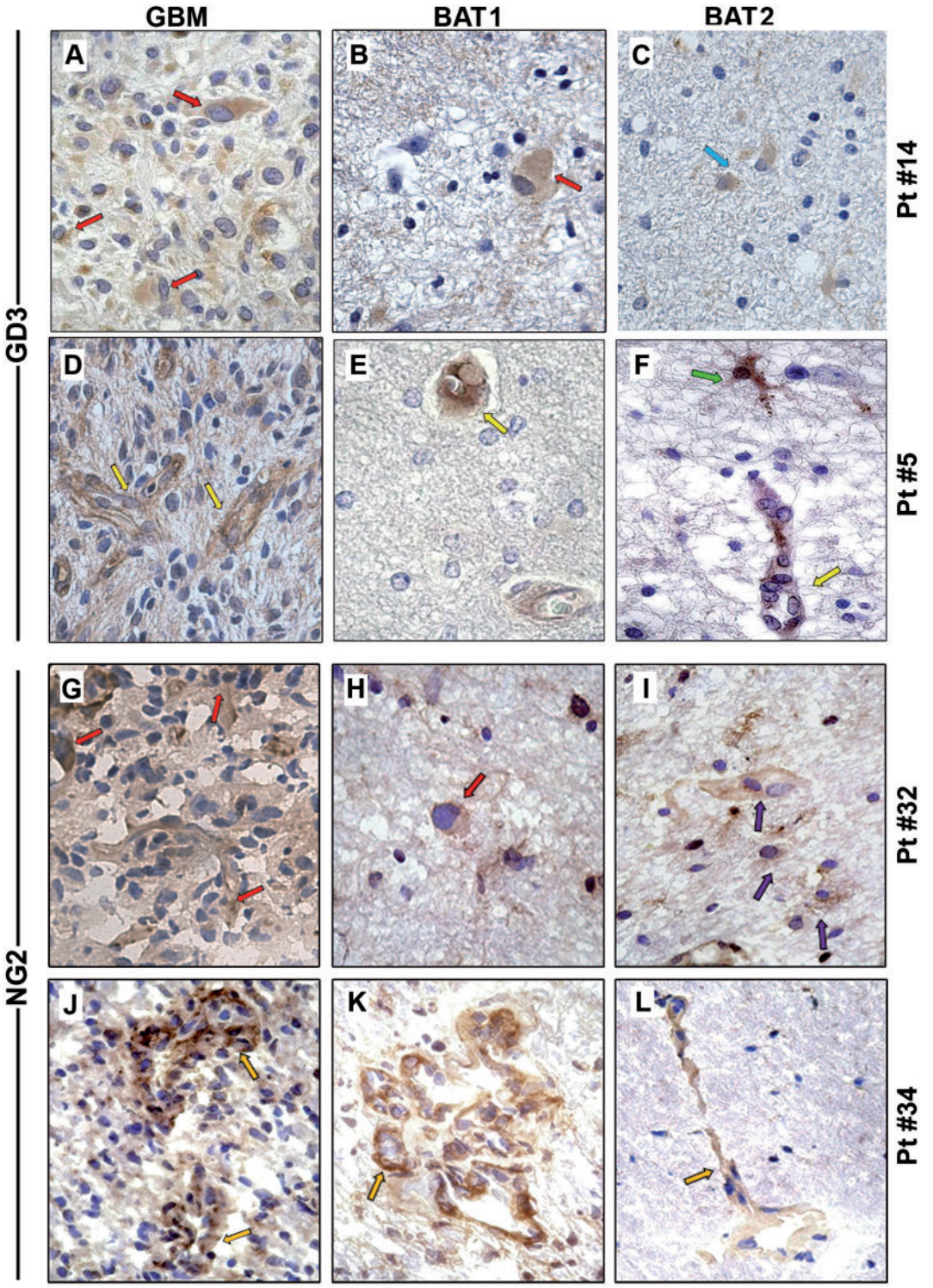

FIGURE 1. Immunohistochemistry of GD3 and NG2 in GBM and BAT. Representative sections from GBM **(A, D, G, J)**, BAT 1 (<1 cm from tumor border) **(B, E, H, K)**, and BAT 2 (≥1 cm from tumor border) **(C, F, I, L)**. GD3 immunoreactivity was detected in the cytoplasm of tumor cells **(A, B**, red arrows**)** and in the endothelium **(D–F**, yellow arrows**)**. Hypertrophic endothelial cells protruding into the microvessel lumen are shown in (**E**). GD3 immunostaining was present in apparently normal cells **(C**, turquoise arrow**)** and reactive astrocytes **(F**, green arrow**)**. NG2 immunoreactivity was present in the cytoplasm of both neoplastic cells **(G, H**, red arrows**)** and glial cells of various morphology **(I**, violet arrows**)**; NG2 was expressed in pericytes (orange arrow) of hyperplastic vessels in the GBM **(J)** and BAT 1 **(K)** as well as in the microvessels of BAT 2 **(L)**. Original magnifications: **A–F, G–I,** x630; **J–L**, x400.

coexpression of α-SMA and NG2, which were largely colocalized in vessel walls (Fig. 2I, GBM; Fig. 2L, BAT). The intermediate filament protein nestin, which is typical for neural stem/precursor cells, appeared to be present in endothelia of GBM vessels (Fig. 2N, O). In BAT, in addition to endothelial cell localization, nestin was found in pericytes where it was coexpressed with NG2 (Fig. 2R). As expected, many cells showed immunoreactivity for NG2 and nestin (Fig. 2A, N) in tumors, whereas less NG2- or nestin-positive elements seemed to be present in BAT (Fig. 2D, J, P, Q).

Ki67 in GBM and in BAT

Ki67 immunoreactivity was intense and was confined to cell nuclei both in GBM and BAT. In the tumors, the numbers of Ki67-positive cells varied between 10% and 60%. When neoplastic-appearing cells were present in BAT 1 and BAT 2, the percentage of labeled cells ranged from 2% to 6%, whereas when neoplastic-appearing cells were not observed, the Ki67 labeling ranged from 0% to 2%. In controls, Ki67-positive cells were extremely rare (Supplementary Data - Figure 2).

PTEN Deletion and MDM2 Amplification in GBM and in BAT

All cases analyzed by FISH had detectable and evaluable nuclear signals. In tumor and in BAT tissue, each sample was mosaic for the disomy (2 hybridization signals), heterozygous (1 hybridization signal), or homozygous *PTEN* deletion (no hybridization signals) (Fig. 3A). The number of nuclei showing the heterozygous or homozygous deletion was higher in tumor (mean = 78.5%) with respect to BAT 1 and BAT 2 (mean = 48% and 38.7%, respectively). In particular, 2 GBM samples showed the highest rate of nuclei with the loss of both copies of the gene (72%, and 58%, respectively). The same analysis performed on control samples showed a normal hybridization pattern in all 50 consecutive nuclei analyzed. Duplication (dup; 3 signals) and amplification (amp; ≥4 signals) of *MDM2* signal (Fig. 3B) were detected in all samples but not in the controls. In the tumors, the dup/amp was observed in 46% of cells and a similar percentage of cells with dup/amp was found in BAT 1 (42.7%) and BAT 2 (46%).

Survival Analysis

Thirty-six patients were included in the Kaplan-Meier analysis; the 4 patients who did not receive radiochemotherapy were excluded (Table 1). This analysis indicated that KPS and gender were not associated with survival time. Furthermore, no association was observed between GD3 expression in the 3 areas and survival time (Supplementary Data - Figure 3A). The only parameter that significantly correlated with survival was age. The median survival time was longer for patients <65 years of age with respect to patients ≥65 years of age (15 vs. 13 months; p = 0.03 log-rank test) (Supplementary Data - Figure 3B).

GCSCs and PCSCs Express NG2 and GD3

GCSCs and PCSCs are endowed with the full spectrum of functional characteristics expected from neural stem cells, such as long-term expansion, self-renewal, and multipotency. The differentiation capability, assessed by immunocytochemistry, was confirmed by the expression of neuronal (β-III-tubulin), astroglial (GFAP), and oligodendroglial (galactocerebrosidase) markers (data not shown).

Immunocytochemical analysis also demonstrated that both GCSCs and PCSCs expressed NG2 and GD3. In particular, GD3 immunoreactivity was present mainly at the membrane level. No relevant difference between the 2 cell populations was observed (Fig. 4A, B, top panel). NG2 was present in the cellular cytoplasm and membrane and staining appeared more intense in GCSCs compared with PCSCs, suggesting higher expression levels (Fig. 4C, D, top panel). Moreover, double-staining immunofluorescence of GD3 and NG2 showed that cells coexpressed both molecules (Fig. 4, bottom panel). Both cell populations expressed Ki67 in the nuclei; GCSCs seemed to show a greater number of immunopositive cells than PCSCs (Supplementary Data - Figure 4A, B).

In the same population, NG2 and GD3 synthase expression was analyzed at the mRNA and protein level by qPCR and Western blotting, respectively. These analyses showed that NG2 and GD3 synthase were expressed in both GCSCs and PCSCs, but NG2 mRNA was present at lower levels in PCSCs compared with GCSCs (Fig. 5A). The differences were also seen in the immunoblotting results (Fig. 5B). Differences in the expression of GD3 synthase transcript between the 2 cell

TABLE 2. GD3 Expression in Brain Tissue Adjacent to Glioblastoma Is Dependent on the Presence of Neoplastic Cells

		BAT 1 With Tumor Cells	BAT 1 Without Tumor Cells	BAT 2 With Tumor Cells	BAT 2 Without Tumor Cells
Number of samples		13	21	8	15
GD3	Median %	5.32	1.36*	8.25	1.04**
	Range	1.0–17.0	0.10–10.20	3.30–14.0	0.16–7.0

BAT, brain tissue adjacent to glioblastoma; BAT 1 (<1 cm from the macroscopic tumor border) with tumor cells derived from patients #5, 8, 13–16, 23, 27–29, 32, 36, and 38; BAT 1 without tumor cells derived from patients #2, 4, 9–12, 17–22, 25, 26, 30, 33–35, 37, 39, and 40. BAT 2 (between 1 and 3.5 cm from the macroscopic tumor border) with tumor cells derived from patients #1, 7, 8, 23, 31, 32, 34, and 35; BAT 2 without tumor cells derived from patients #3, 5, 6, 10, 11, 12, 14, 15, 17, 20–22, 24, 30, and 33.

*p = 0.002, BAT 1 with vs. BAT 1 without tumor cells, Mann-Whitney test; **p = 0.001, BAT 2 with vs. BAT 2 without tumor cells, Mann-Whitney test.

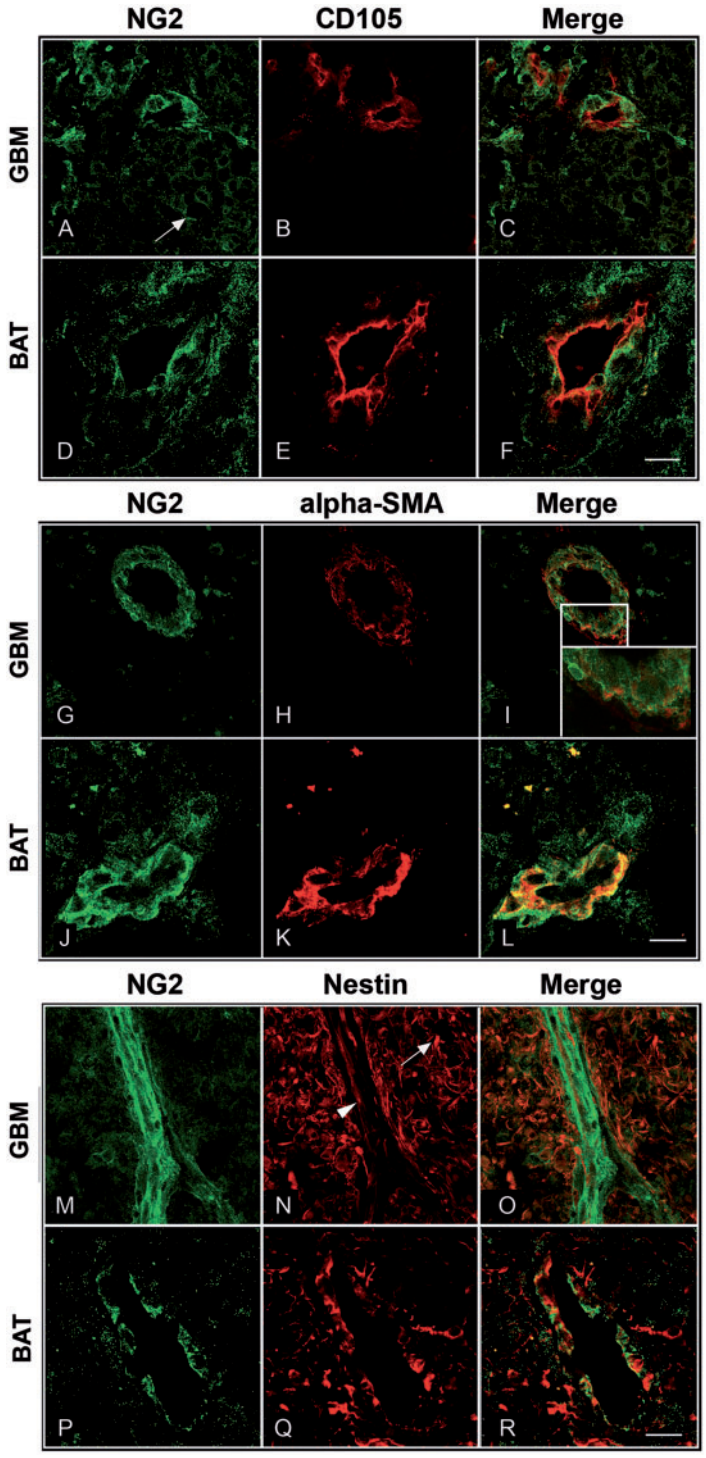

FIGURE 2. Double-label fluorescent immunohistochemistry in GBM and BAT samples. Confocal microscopy micrographs of representative samples from GBM and BAT showing NG2 **(A, D, G, J, M, P**, green**)**, CD105 **(B, E)**, α-SMA **(H, K)**, and nestin **(N, Q,** red**)** expression. In both GBM and BAT, the neo-angiogenesis marker CD105 was expressed by endothelial cells **(B, C, E, F)**, whereas the markers NG2 and α-SMA were expressed by pericytes **(G–L)**. The inset taken from the boxed region in **I** (GBM) shows, at higher magnification, the expression of the 2 markers in different cytoplasmic compartments of pericytes, whereas **L** (BAT) indicates the colocalization of the 2 markers in pericytic cells. In GBM **(N)**, nestin was mainly detected in the majority of cancer cells (arrow) and endothelial cells (arrowhead). In GBM, NG2 and nestin do not colocalize in the vessel wall, whereas sporadic NG2 expression is detectable in nestin-positive tumor cells **(O)**. In BAT, nestin, besides the endothelial localization **(O)**, was found coexpressed with NG2 in pericytes **(R)**. Scale bars: **A–F, G–I, M–O**, 30 μm; **J–L**, 20 μm; **P–R**, 15 μm. GBM and BAT frozen tissues were obtained from patient #23.

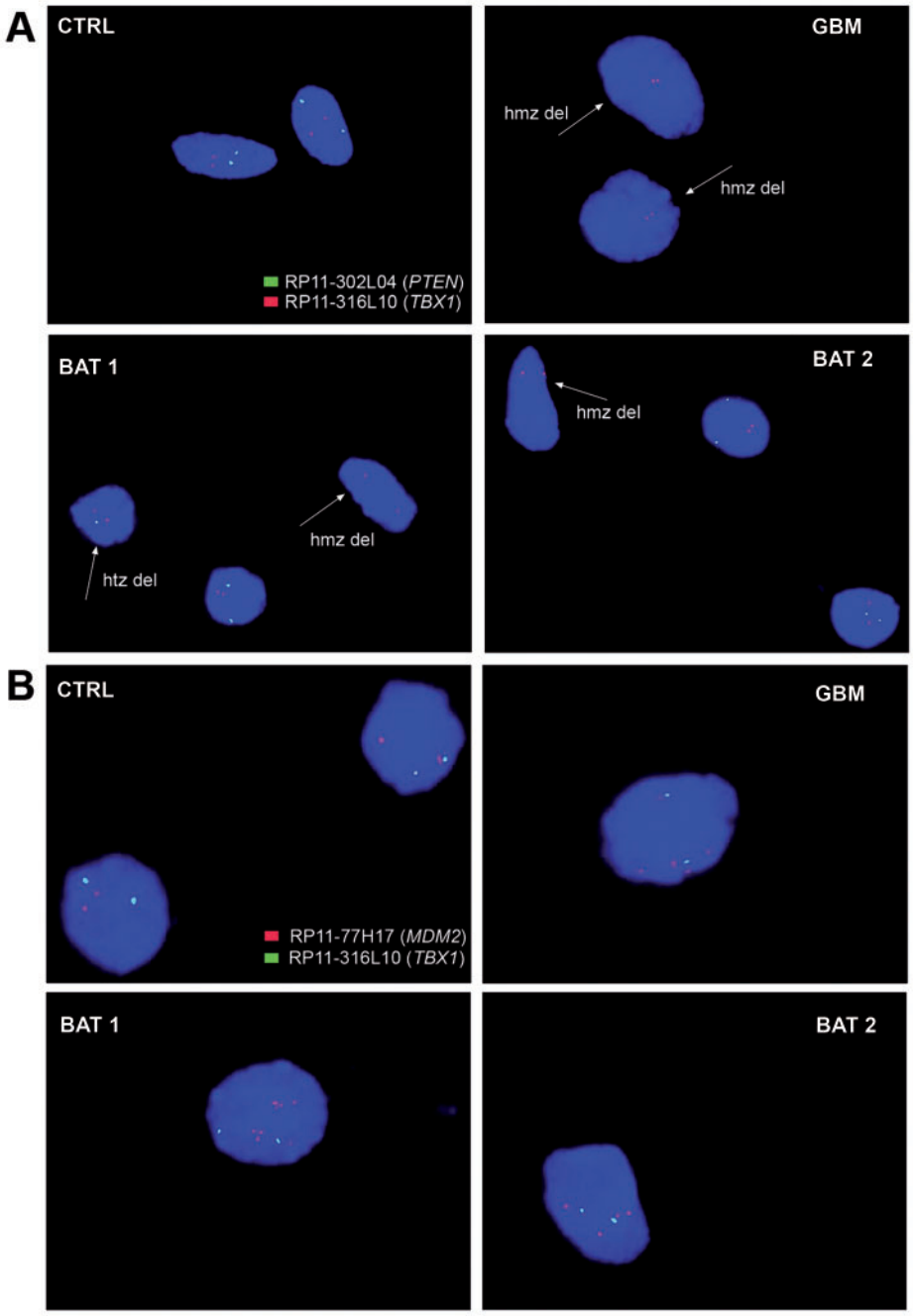

FIGURE 3. FISH-mediated detection of*PTEN* deletion and*MDM2* amplification in GBM and in BAT. A representative case of FISH analysis performed on nuclei isolated from paraffin-fixed, formalin-embedded specimens from GBM, BAT 1, and BAT 2. **(A)** Mosaic *PTEN* deletion (heterozygous: htz or homozygous: hmz). The RP11-302L04 (green signals) clone that includes *PTEN* gene was used. RP11-316L10 (red signals) clone, mapping to 22q11.21, was used as control. Top left: nuclei isolated from a control (CTRL) show a normal hybridization pattern for *PTEN* probe (green signals). Top right: 2 nuclei isolated from GBM showing both the loss of the 2 copies of *PTEN* (arrow with hmz del). Bottom left: FISH analysis in the BAT 1 showing 1 normal nucleus, 1 with the heterozygous *PTEN* deletion (arrow with htz del), and another with the homozygous deletion (arrow with hmz del). Bottom right: 2 nuclei from BAT 2 with a normal hybridization pattern and 1 with the homozygous deletion (arrow with hmz del). Cells derived from GBM, BAT 1, and BAT 2 were obtained from paraffin-embedded tissues of patient #30. **(B)** *MDM2* Amplification. The RP11-77H17 clone (red signal), which includes the *MDM2* gene, was used. In all samples, RP11-310L10 clone mapping to 22q11.21 and green labeled was used as control probe. Top left: FISH on nuclei isolated from a CTRL shows a normal hybridization pattern with 2 red signals representing 2 copies of *MDM2*. Top right and left and right below: nuclei from the tumor, BAT 1 and 2 show more than 2 red signals, indicating the amplification of *MDM2* gene. Cells of GBM, BAT 1, and BAT 2 were obtained from paraffin-embedded tissues of patient #30.

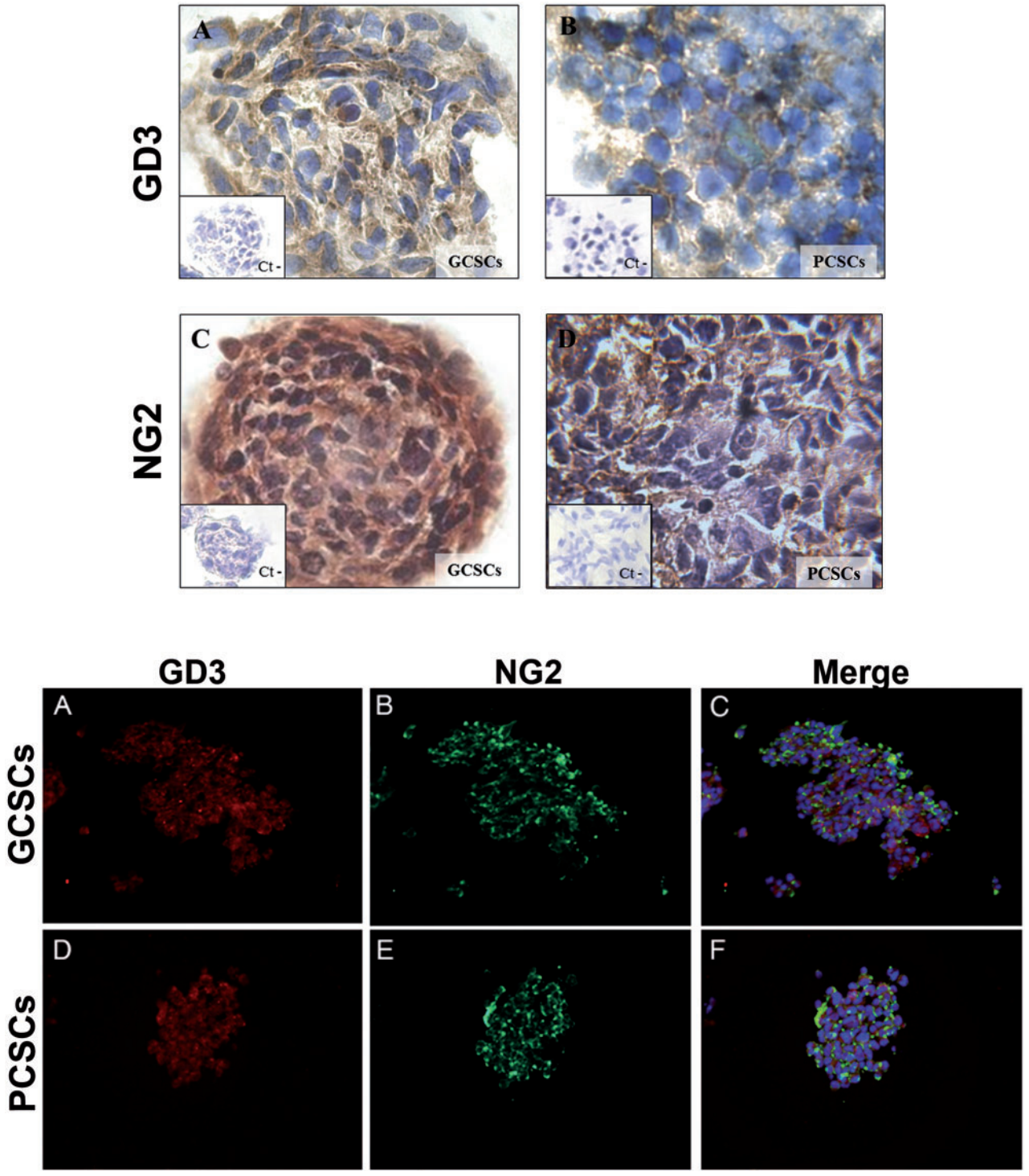

FIGURE 4. GD3 and NG2 expression in GCSCs and PCSCs evaluated by immunocytochemistry. Representative images of GCSCs and PCSCs derived from patient #40. Top panel: Immunocytochemistry of GD3 and NG2 in GCSCs and PCSCs. GD3 was expressed in both GCSCs **(A)** and PCSCs **(B)**. GD3 immunoreactivity was mainly detected at the cell membrane level. NG2 expression was detected in both GCSCs **(C)** and PCSCs **(D)**. NG2 immunoreactivity was present in the cytoplasm and at the cell membrane level. The insets represent the negative controls (Ct-) performed by omitting the primary antibody. Original magnification: x630 and x200 (Ct-). Bottom panel: GD3-NG2 double-label fluorescent immunocytochemistry in GCSCs and PCSCs. Representative sections of GCSCs **(A–C)** and PCSCs **(D–F)** neurospheres double stained for GD3 **(**red; **A, D)** and NG2 **(**green; **B, E)**. GCSCs and PCSCs expressed both molecules. Their coexpression was found in a small number of cells **(**merge; **C, F)**. Original magnification: x200.

types of 2/4 patients were significant (Supplementary Data - Figure 5A), whereas, as far as the protein level is concerned, significance was reached in only 1 case (Supplementary Data - Figure 5B).

GCSCs and PCSCs Tumorigenicity in Mice

CSCs isolated from 4 patients formed intracranial tumors in immunocompromised mice. GCSC-derived tumors showed histological characteristics that recapitulated the cytoarchitecture of the parental tumor (Fig. 6A, C, E), whereas PCSC-derived tumors were less vascularized, and their proliferative potential was comparable to that of grade III gliomas (Fig, 6B, D). GCSCs and PCSCs were functionally characterized, and it was found that the former exhibit a higher proliferative potential *in vitro*, which correlated with a higher clonogenicity (data not shown). More importantly, this correlated with a higher tumor-initiating ability when compared with PCSCs, which had

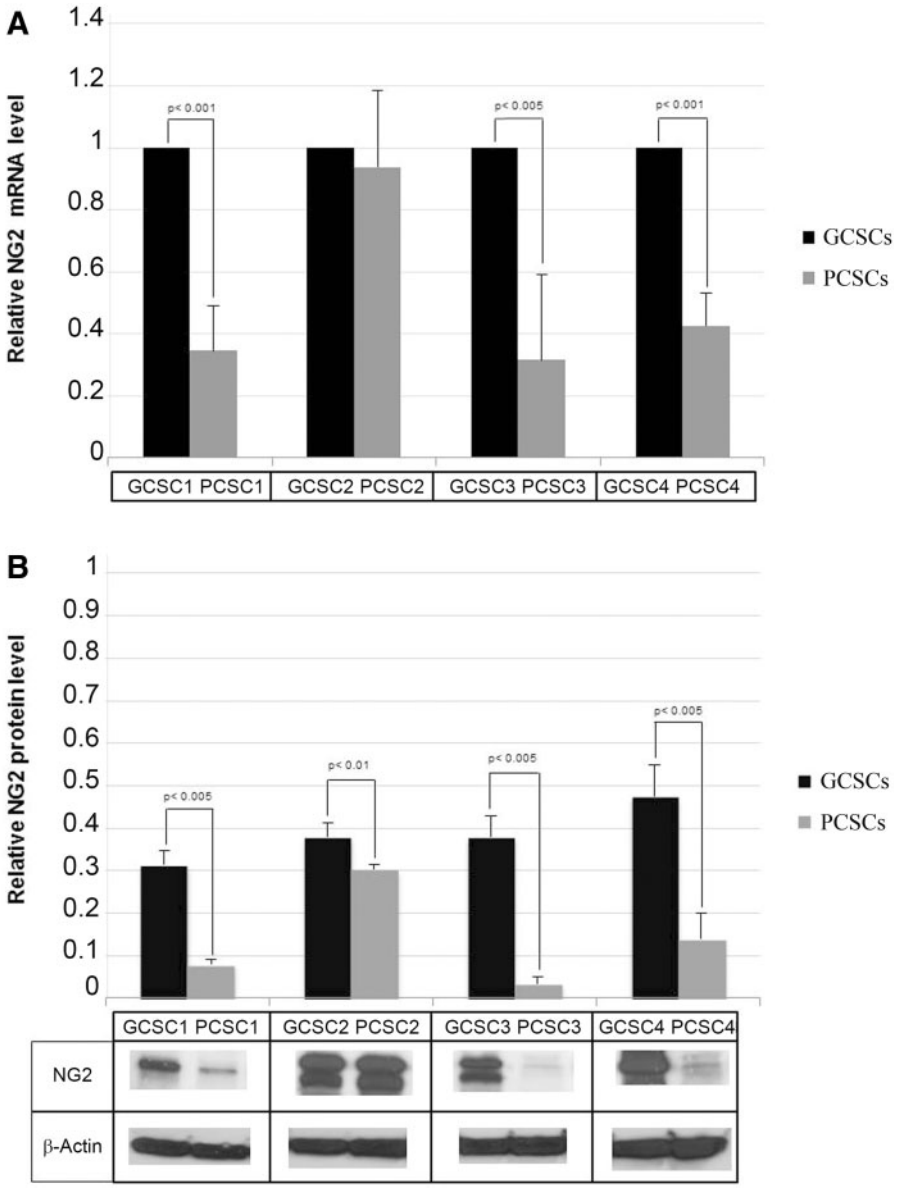

FIGURE 5. Molecular analysis of NG2 expression in GCSCs and PCSCs. **(A)** Evaluation of NG2 mRNA level by qPCR normalized to β-actin in 4 GCSC/PCSC paired samples; GCSC1/PCSC1 were isolated from Patient (Pt) #32, GCSC2/PCSC2 from Pt #38, GCSC3/PCSC3 from Pt #39, GCSC4/PCSC4 from Pt #40). Data show the relative fold change of NG2 transcript in PCSCs vs. GCSCs (set to 1). **(B)** Western blot analysis of NG2 protein expression. Representative immunoblots are shown. Bar graphs show relative density of protein bands normalized to β-actin (used as loading control). The NG2 upper band represents the mature proteoglycan containing chondroitin sulphate, whereas the lower band corresponds to the 300 kDa NG2 core protein. Values represent the mean ± SD of 3 independent experiments. Data were analyzed by Student t-test.

lower tumorigenicity *in vivo*. Animal survival time, investigated by Kaplan-Meier analysis revealed that mice that received GCSCs died significantly earlier (median survival: 74 days) than mice that received PCSCs (median survival: 195 days) ($p < 0.0001$) (Fig. 6F).

DISCUSSION

Here, we have demonstrated the expression of GD3 and NG2 in GBM, BAT, and CSCs isolated from these 2 regions. Our findings on the spatial localization of GD3 and NG2 are in partial agreement with a previous report by Chekenya et al. who described NG2 expression only in the tumor mass while detecting GD3 throughout the GBM tissue to the BAT (36). We found that these markers are localized in neoplastic cells, reactive astrocytes, apparently normal cells, and in GBM and BAT vessel walls. Our findings on GD3 are consistent with previous data (24, 26, 37); in particular, the expression of this marker in human glioma cells seems to be involved in the modulation of cell migration and invasion (24). In addition to various neural cell types, such as oligodendrocyte progenitors, GD3 and NG2 have been shown to be expressed in astrocytes and pericytes associated with tumor microvasculature, respectively (38–40).

In addition, it has been reported that the local recruitment of glial progenitors residing in adult white matter, including NG2-positive cells, can contribute significantly to the GBM proliferative mass and rapid progression. During their abnormal proliferation, some of these cells can acquire genetic alterations and a consequent neoplastic transformation (41). In our experience, GD3- and NG2-positive cells with an apparently normal morphology were detected in BAT at a distance up to 3.5 cm from the tumor edge, irrespective of the presence of infiltrating tumor cells. They might represent progenitor cells that, due to growth factors produced by the tumor mass, may be attracted by glioma cells and contribute to GBM progression. On the other hand, FISH analysis in BAT demonstrated typical GBM genetic alterations such as *PTEN* deletion and *MDM2* amplification, even in the absence of cells with neoplastic morphology, which might represent early genetic modifications leading to the neoplastic transformation in combination with other later mutations and/or epigenetic

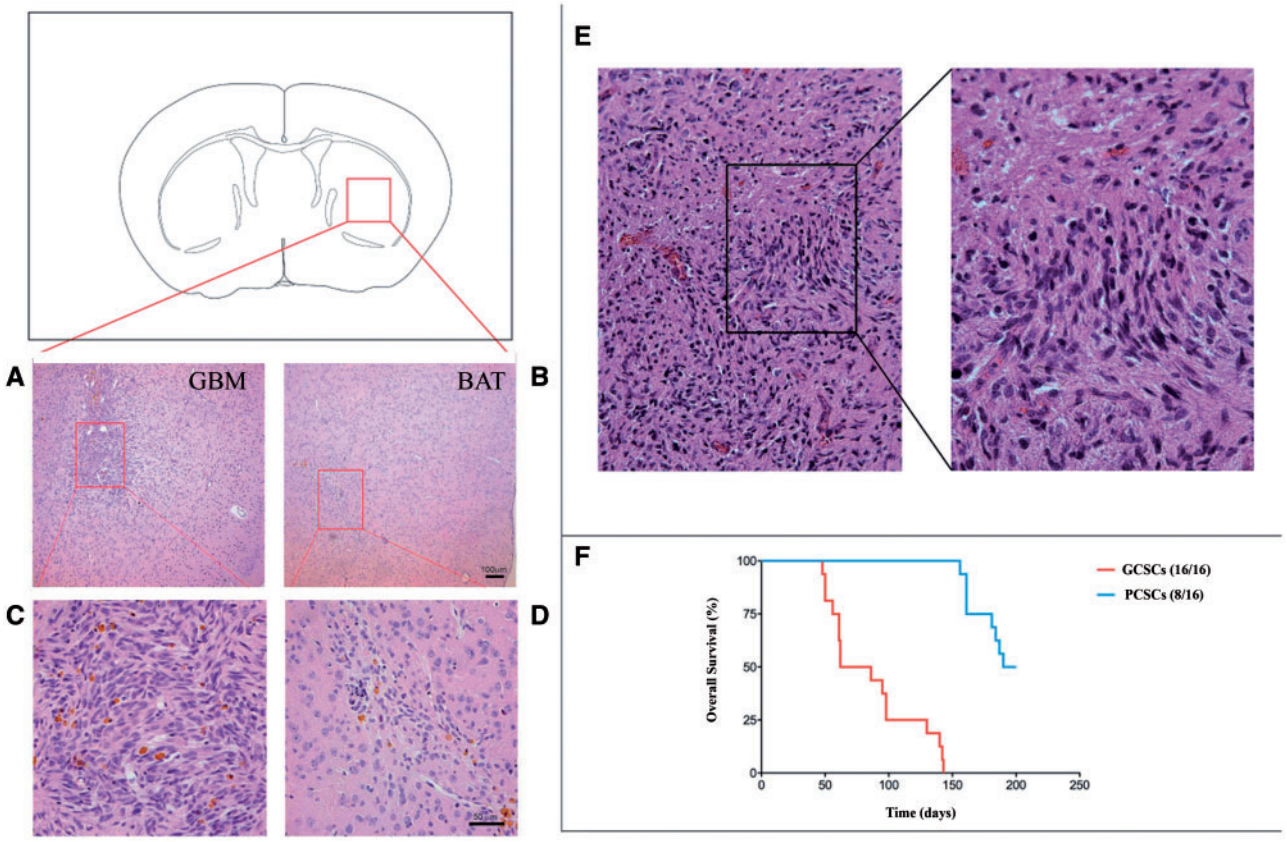

FIGURE 6. Evaluation of *in vivo* tumorigenicity of GCSCs and PCSCs. Representative sections of GCSC **(A)** and PCSC **(B)**-derived tumors stained with H&E (Patient [Pt] #38). Higher magnification showing neoplastic elements in a GCSC-derived tumor **(C)** and few neoplastic cells in a PCSC-derived one **(D)**. The GCSC-derived tumor resembles human original GBM tissue **(E)**. **(F)** Kaplan-Meier survival analysis of*Scid/bg* mice injected with GCSCs and PCSCs (GCSC1/PCSC1 were isolated from Pt #32, GCSC2/PCSC2 from Pt #38, GCSC3/PCSC3 from Pt #39, GCSC4/PCSC4 from Pt #40). Mice receiving GCSCs died significantly earlier (median survival: 74 days) than mice receiving PCSCs cells (median survival: 195 days). Log-rank test, $p < 0.0001$ (GCSCs vs. PCSCs). Scale bars: **A, B**, 100 μm; **C, D**, 50 μm. Original magnification: x200 **(E**, left panel**)**; x400 **(E**, right panel**)**.

alterations. Nevertheless, the nature of cells populating BAT and their crosstalk with their microenvironment is still debated. Previously, we demonstrated that GBM cell invasion of BAT could be considered a prognostic factor for survival. In fact, patients with tumor cells in the GBM neighboring tissue had a shorter survival (29). The amount of GD3-positive cells we found in BAT might be associated with malignant cell infiltration, supporting previous reports that indicate a correlation of GD3 expression with a migratory phenotype (42). In addition, GD3 is involved in the proliferation of mouse neural stem cells through the activation of ERK1/2 (43), which, in our experience, is expressed not only in tumor but also in BAT (14).

We have shown GD3 expression in endothelial cells of both tumor and BAT, suggesting that this ganglioside is also involved in neoangiogenesis, probably as an indirect factor. Indeed, gangliosides prompt both the migration of endothelial cells (44) and the release of vascular endothelial growth factor by GBM cells (25). A critical role in supporting vascular structure and function, vessel maturation, and vessel sprouting initiation is played by pericytes that express NG2 (39). In our study, NG2-positive pericytes were detected in the vessel walls of both tissue compartments. Notably, in BAT, NG2 and nestin were coexpressed in these cells, also in the absence of tumor cells. It has been demonstrated that nestin-positive mesenchymal stem cells also express NG2 and differentiate into pericyte-like mural cells when exposed to GBM cell conditioned medium (45). Since it has been hypothesized that GBM recruits mesenchymal progenitor cells from bone marrow by secretion of angiogenic factors and chemokines (46), our findings seem to indicate that the NG2- and nestin-expressing cells may be derived from recruited mesenchymal stem cells. NG2 was found to be downregulated in pericytes associated with quiescent vessels of normal brain tissue (39). Thus, our data support the occurrence of neoangiogenic processes in BAT. Interestingly, this is in line with recent findings suggesting that only a specific type of pericytes, expressing both nestin and NG2, is recruited during tumor angiogenesis (47). Moreover, some authors propose that these cells might derive from CSCs in GBM (48). Neoangiogenesis in BAT is also supported by the presence of CD105-positive endothelial cells in a microvascular niche, as previously demonstrated (19), because this molecule seems to represent a specific marker of tumor-associated blood vessels (18) as well as a marker for mesenchymal stem cells (49). The presence of CSCs in BAT showing features different from those derived from the tumors further highlight the relevance of GBM-surrounding tissue in tumor growth and development. In this regard, Piccirillo et al. detected 2 types of CSCs that differed in both genetic alterations and tumor-initiating ability in GBM and in tissue from at least 2 cm from tumor border (22).

In a recent study, these authors found that CSCs derived from the tumor mass were tumorigenic *in vivo* and self-renewing *in vitro*, whereas those derived from GBM peritumor tissue were tumorigenic *in vivo* but had lost their self-renewal capacity *in vitro* (50). Glas et al. described distinct BAT-derived malignant subentities (defined as residual tumor cells), showing an increased proliferation/invasiveness rate, a reduction in self-renewal capacity, and different patient-related responses to radiation and/or chemotherapy, compared with their paired-GBM-derived CSCs (51). We found that PCSCs expressing low levels of NG2 showed a lower Ki67 level and a reduced growth rate when compared with GCSCs, and, in disagreement with data reported by other authors (50, 51), they maintained the self-renewal capacity *in vitro*. In our experience, a decline of nuclear Ki67 staining is found at the boundary between GBM and neighboring tissue. This interface is a critical invasion area where many proliferating cell types, barely distinguishable, are present, in addition to migrating neoplastic cells.

Interestingly, we observed that tumors derived from low NG2-expressing PCSCs showed a less aggressive behavior compared with the high NG2 expressing GCSC-derived ones. In fact, PCSC-resulting tumors allowed mice to survive for a longer time. Indeed, PCSC-derived tumors are less vascularized and their proliferative potential is comparable to that of grade III gliomas (22). In this regard, Wang and colleagues reported that NG2 overexpressing GBM cells implanted into nude rat brains triggered tumors showing increased growth rate, angiogenesis, and vascular permeability. By contrast, shRNA-mediated silencing of NG2 in GBM-derived cells led to reduced tumor growth, edema, and angiogenesis (52). We did not find any relationship between GD3 synthase expression and mice survival. Given the comparable enzyme levels detected in both PCSCs and GCSCs, this is not surprising. The coexpression of GD3 and NG2 in a subset of GCSCs and PCSCs seems to characterize a cell population, which might represent cells with stemness property and tumor initiation-propagation ability.

Altogether, our findings demonstrate that, up to the remarkable distance of 3.5 cm from the tumor margin, BAT shows GD3 and NG2 expression, as well as *PTEN* and *MDM2* mutations despite the absence of cells with morphological features of neoplastic transformation. These results corroborate the idea that pre/pro-tumorigenic events might occur in this tissue and that among the involved cells, some might be endowed with a cancer stem cell-like phenotype. Lastly, these findings provide a further insight in the complexity of GBM-neighboring microenvironment which plays a crucial role in tumor progression.

REFERENCES

1. Parsons DW, Jones S, Zhang X, et al. An integrated genomic analysis of human glioblastoma multiforme. Science 2008;321:1808–12
2. McDonald KL, Aw G, Kleihues P. Role of biomarkers in the clinical management of glioblastomas: What are the barriers and how can we overcome them? Front Neurol 2012;3:1–8
3. Furnari FB, Fenton T, Bachoo RM, et al. Malignant astrocytic glioma: Genetics, biology, and paths to treatment. Genes Dev 2007;212:683–710
4. Hochberg FH, Pruitt A. Assumptions in the radiotherapy of glioblastoma. Neurology 1980;30:907–11
5. Park I, Tamai G, Lee MC, et al. Patterns of recurrence analysis in newly diagnosed glioblastoma multiforme after three-dimensional conformal radiation therapy with respect to pre-radiation therapy magnetic resonance spectroscopic findings. Int J Radiat Oncol Biol Phys 2007;69:381–9
6. Bakshi A, Nag TC, Wadhwa S, et al. The expression of nitric oxide synthases in human brain tumours and peritumoral areas. J Neurol Sci 1998;155:196–203
7. Roy S, Sarkar C. Ultrastuctural study of micro-blood vessels in human brain tumors and peritumoral tissue. J Neurooncol 1989;7:283–94
8. Lorger M. Tumor microenvironment in the brain. Cancers 2012;4:218–43

9. Charles NA, Holland EC, Gilbertson R, et al. The brain tumor microenvironment. Glia 2012;60:502–14
10. Dehnhardt M, Zoriy MV, Khan Z, et al. Element distribution is altered in a zone surrounding human glioblastoma multiforme. J Trace Elem Med Biol 2008;22:17–23
11. Melani A, De Micheli E, Pinna G, et al. Adenosine extracellular levels in human brain gliomas: An intraoperative microdialysis study. Neurosci Lett 2003;346:93–6
12. Cubillos S, Obregón F, Vargas MF, et al. Taurine concentration in human gliomas and meningiomas: Tumoral, peritumoral, and extratumoral tissue. Adv Exp Med Biol 2006;583:419–22
13. Haybaeck J, Obrist P, Schindler CU, et al. STAT-1 expression in human glioblastoma and peritumoral tissue. Anticancer Res 2007;27: 3829–35
14. Lama G, Mangiola A, Anile C, et al. Activated ERK1/2 expression in glioblastoma multiforme and in peritumor tissue. Int J Oncol 2007; 30:1333–42
15. Mangiola A, Lama G, Giannitelli C, et al. Stem cell marker nestin and c-Jun NH2-terminal kinases in tumor and peritumor areas of glioblastoma multiforme: Possible prognostic implications. Clin Cancer Res 2007; 13:6970–7
16. Ehrmann J, Kolár Z, Mokry J. Nestin as a diagnostic and prognostic marker: Immunohistochemical analysis of its expression in different tumours. J Clin Pathol 2005;58:222–3
17. Lendahl U1, Zimmerman LB, McKay RD. CNS stem cells express a new class of intermediate filament protein. Cell 1990;60:585–95
18. Dallas NA, Samuel S, Xia L, et al. Endoglin (CD105): A marker of tumor vasculature and potential target for therapy. Clin Cancer Res 2008; 14:1931–7
19. Sica G, Lama G, Anile C, et al. Assessment of angiogenesis by CD105 and nestin expression in peritumor tissue of glioblastoma. Int J Oncol 2011;38:41–9
20. Mangiola A, Saulnier N, De Bonis P, et al. Gene expression profile of glioblastoma peritumoral tissue: An ex vivo study. PLoS One 2013;8: e57145
21. Singh SK, Hawkins C, Clarke ID, et al. Identification of human brain tumour initiating cells. Nature 2004;432:396–401
22. Piccirillo SG, Combi R, Cajola L, et al. Distinct pools of cancer stem-like cells coexist within human glioblastomas and display different tumorigenicity and independent genomic evolution. Oncogene 2009;28: 1807–11
23. Al-Mayhani MT, Grenfell R, Narita M, et al. NG2 expression in glioblastoma identifies an actively proliferating population with an aggressive molecular signature. Neuro Oncol 2011;13:830–45
24. Merzak A, Koochekpour S, Pilkington GJ. Adhesion of human glioma cell lines to fibronectin, laminin, vitronectin and collagen I is modulated by gangliosides in vitro. Cell Adhes Commun 1995;3:27–43
25. Koochekpour S, Merzak A, Pilkington GJ. Vascular endothelial growth factor production is stimulated by gangliosides and TGF-beta isoforms in human glioma cells in vitro. Cancer Lett 1996;19:209–15
26. Koochekpour S, Pilkington GJ. Vascular and perivascular GD3 expression in human glioma. Cancer Lett 1996;104:97–102
27. Chow LM, Baker SJ. PTEN function in normal and neoplastic growth. Cancer Lett 2006;241:184–96
28. Zhao Y, Yu H, Hu W. The regulation of MDM2 oncogene and its impact on human cancers. Acta Biochim Biophys Sin 2014;46:180–9
29. Mangiola A, De Bonis P, Maira G, et al. Invasive tumor cells and prognosis in a selected population of patients with glioblastoma multiforme. Cancer 2008;113:841–6
30. Hoelzinger DB, Mariani L, Weis J, et al. Gene expression profile of glioblastoma multiforme invasive phenotype points to new therapeutic targets. Neoplasia 2005;7:7–16
31. Stupp R, Mason WP, van den Bent MJ, et al. Radiotherapy plus concomitant and adjuvant temozolomide for glioblastoma. N Engl J Med 2005; 352: 987–96
32. Binda E, Visioli A, Giani F, et al. The EphA2 receptor drives self-renewal and tumorigenicity in stem-like tumor-propagating cells from human glioblastomas. Cancer Cell 2012;22:765–80
33. Galli R, Binda E, Orfanelli U, et al. Isolation and characterization of tumorigenic, stem-like neural precursors from human glioblastoma. Cancer Res 2004;64:7011–21
34. Bernardini L, Giuffrida MG, Francalanci P, et al. X chromosome monosomy restricted to the left ventricle is not a major cause of isolated hypoplastic left heart. Am J Med Genet A 2010;152A:1967–72
35. Livak KJ, Schmittgen TD. Analysis of relative gene expression data using real-time quantitative PCR and the 22DDCT method. Methods 2001;25:402–8
36. Chekenya M, Enger PØ, Thorsen F, et al. The glial precursor proteoglycan, NG2, is expressed on tumour neovasculature by vascular pericytes in human malignant brain tumours. Neuropathol Appl Neurobiol 2002; 28:367–80
37. Kawai K, Watarai S, Takahashi H, et al. Demonstration of ganglioside GD3 in human reactive astrocytes. Psychiatry Clin Neurosci 1999;53:79–82
38. Goldman JE, Reynolds R. A reappraisal of ganglioside GD3 expression in the CNS. Glia 1996;16:291–5
39. Stallcup WB, Huang FJ. A role for the NG2 proteoglycan in glioma progression. Cell Adhes Migr 2008;2:192–201
40. Zhu L, Lu J, Tay SS, et al. Induced NG2 expressing microglia in the facial motor nucleus after facial nerve axotomy. Neuroscience 2010;166:842–51
41. Assanah M, Lochhead R, Ogden A, et al. Glial progenitors in adult white matter are driven to form malignant gliomas by platelet-derived growth factor-expressing retroviruses. J Neurosci 2006;26:6781–90
42. Ohkawa Y, Momota H, Kato A, et al. Ganglioside GD3 enhances invasiveness of gliomas by forming a complex with platelet-derived growth factor receptor α and Yes kinase. J Biol Chem 2015;290:16043–58
43. Jung JU, Ko K, Lee DH, et al. The roles of glycosphingolipids in the proliferation and neural differentiation of mouse embryonic stem cells. Exp Mol Med 2009;41:935–45
44. Alessandri G, Raju KS, Cullino PM. Interaction of gangliosides with fibronectin in the mobilization of capillary endothelium. Possible influence on metastasis. Invasion Metastasis 1986;6:145–65
45. Birnbaum T, Hildebrandt J, Nuebling G, et al. Glioblastoma-dependent differentiation and angiogenic potential of human mesenchymal stem cells in vitro. J Neurooncol 2011;105:57–65
46. Birnbaum T, Roider J, Schankin CJ, et al. Malignant gliomas actively recruit bone marrow stromal cells by secreting angiogenic cytokines. J Neurooncol 2007;83:241–7
47. Birbrair A, Zhang T, Wang ZM, et al. Type-2 pericytes participate in normal and tumoral angiogenesis. Am J Physiol Cell Physiol 2014;307:C25–38
48. Cheng L, Huang Z, Zhou W, et al. Glioblastoma stem cells generate vascular pericytes to support vessel function and tumor growth. Cell 2013; 28:139–52
49. Chamberlain G, Fox J, Ashton B, et al. Concise review: Mesenchymal stem cells: their phenotype, differentiation capacity, immunological features, and potential for homing. Stem Cells J 2007;25:2739–49
50. Piccirillo SG, Dietz S, Madhu B, et al. Fluorescence-guided surgical sampling of glioblastoma identifies phenotypically distinct tumour-initiating cell populations in the tumour mass and margin. Br J Cancer 2012;107:462–8
51. Glas M, Rath BH, Simon M, et al. Residual tumor cells are unique cellular targets in glioblastoma. Ann Neurol 2010;68:264–9
52. Wang J, Svendsen A, Kmiecik J, et al. Targeting the NG2/CSPG4 proteoglycan retards tumour growth and angiogenesis in preclinical models of GBM and melanoma. PLoS One 2011;6:e23062